Micro- and nanofibers and liquid crystals for light-scattering shutters: Simulation of electro-optical properties

P. L. Almeida,[1,*] M. H. Godinho,[2,†] and J. L. Figueirinhas[3,‡]

[1]*Area Departamental de Física, Instituto Superior de Engenharia de Lisboa, ISEL/IPL, R. Conselheiro Emídio Navarro, 1, 1950-062 Lisboa, Portugal*
and I3N–CENIMAT, Faculdade de Ciências e Tecnologia, FCT/UNL, 2829-516 Caparica, Portugal

[2]*Departamento de Ciência dos Materiais and I3N–CENIMAT, Faculdade de Ciências e Tecnologia, FCT/UNL, 2829-516 Caparica, Portugal*

[3]*Departamento de Física, Instituto Superior Técnico, IST/UTL, Avenida Rovisco Pais, 1049-001 Lisboa, Portugal*
and CFMC–UL, Avenida Prof. Gama Pinto 2, 1649-003 Lisboa, Portugal

(Received 28 October 2013; published 23 January 2014)

This work demonstrates the feasibility of using polymeric micro- and nanofiber-composed films and liquid crystals as electrically switchable scattering light shutters. We present a concept of electro-optic device based on an innovative combination of two mature technologies: optics of nematic liquid crystals and electrospinning of nanofibers. These devices have electric and optical characteristics far superior to other comparable methods. The simulation presented shows results that are highly consistent with those of experiments and that explain the working mechanism of the devices.

DOI: 10.1103/PhysRevE.89.012507 PACS number(s): 61.30.Pq, 42.79.Kr, 61.30.Gd, 78.35.+c

I. INTRODUCTION

Liquid crystals (LCs) have been widely used as light modulators [1]. The effective refractive index of LCs can be changed significantly by applying a substantially lower field than is required to modulate the refractive index of other materials. Also, LCs are highly transparent in the visible and near-infrared wavelength regions, and so can be used as modulators, switches, shutters, and wavelength filters for optical communication.

Cellulose derivative composites for electro-optical application were introduced in 1982 by Craighead and coworkers [2], followed a few years later by the development of a cellulose derivative electro-optical device named cellulose based polymer dispersed liquid crystal (CPDLC) [3,4]. Recently an innovative solution with optimized electro-optical performance and reduced production cost was presented [5] where light-scattering electro-optical devices were produced with two layers of a cellulose derivative deposited as a nonwoven nano- and microfiber mat onto the conductive substrates by electrospinning and a nematic LC.

These devices represent an important new class of materials for optical device applications [6–8]. These inhomogeneous polymer-LC composites have a spatially varying effective refractive index and efficiently scatter light, which makes them translucent. Light scattering is switched off by simply applying an electric field across the film to reorient the LCs. In this state the film becomes transparent. Being so, these devices require no extra optical elements (other than optically transparent electrodes) to provide optical contrast. Because small current flows are involved in energizing these devices, they also consume relatively low power. As a result, they are particularly suited to be used in low cost large-area applications and are already used in electrically switchable windows.

In the past, different simulations have been used to study light-scattering devices loosely related to ours, namely, polymer dispersed liquid crystals (PDLC), in a variety of physical situations such as different droplet dimensions, director configurations, different boundary conditions [9], and anchoring strengths at the nematic-polymer interface [10,11]. Other extensively studied light-scattering systems with relations to ours include confined LCs with internal disorder induced by aerosil or aerogel [12–14]. The different morphology of our system requires a specific model to address the light-scattering problem. The model simulations provide a key test to the working mechanism of this device and are an important asset in the design of a better performing electro-optical cell.

II. RESULTS AND ANALYSIS

In this work we simulate the electro-optical response of a device composed by a micro- and nanometric fiber assembly as shown in Fig. 1. Both the production and the characterization performed to obtain the electro-optical data are described somewhere else [5].

The fact that the liquid crystal is not confined in droplets or placed in layers, but is interpenetrating a network of fibers gives rise to enhanced electro-optical properties of the devices. These improvements come from the fact that the polymer is acting as a stabilizer of the liquid crystal and since the fibers are randomly distributed, the orientation of the liquid crystal director in the OFF state close to the polymer-LC interfaces is also random, improving the scattering characteristics of this state.

Due to the good match between the ordinary refractive index of the liquid crystal E7 (1.510) and the refractive index of CA (1.45) a very clear ON state is achieved when an electric

*palmeida@adf.isel.pt
†mhg@fct.unl.pt
‡figuei@cii.fc.ul.pt

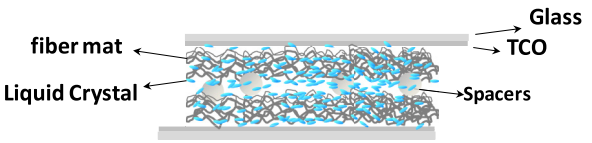

FIG. 1. (Color online) Schematic representation of the device's assembly.

field E_{on} is applied to the device and the director aligns with the field.

To simulate the electro-optical characteristics of these devices we consider a model for an idealized cell where the nematic LC is confined to a layer in between the two polymer film layers arising from the fiber deposition over the transparent conducting substrates. Light passing through the device at different points suffers a phase shift that may vary significantly from point to point over the illuminated area depending upon the orientation of the nematic liquid crystal director, the refractive indices of the liquid crystal and the polymer, and the local surfaces features. For polymer surface features in the micron range and due to the similarity between the refractive indices involved, the scattering problem may be considered to fall within the anomalous diffraction conditions [15], and in this case the light wave electric field at the detector is calculable from Kirchhoff's diffraction theory [16] with a position dependent phase shifted incident field over the illuminated area.

The nematic director field in the LC layer is determined from the solution of the appropriate dynamic equations for the director obtained from the Leslie-Erickson theory of nematodynamics and neglecting fluid flow, this is equivalent to saying that the director field is determined through the minimization of the free energy composed of a Frank elastic term plus an electric term and subjected to the boundary conditions at the polymer-LC interfaces assuming strong boundary conditions [17]. These interfaces are rough with a random nature and will locally determine the director orientation, but on average the director seems to adopt a planar orientation close to these surfaces as suggested by the data analysis. In the simplified model we consider, for the determination of the overall director field, the surface details are disregarded and uniform strong planar anchoring conditions with a small pretilt θ_1 are used. It is also considered that the director only varies with the distance to the LC-polymer interfaces (z distance to one LC-polymer interface) and may experience a twist on going from one LC-polymer interface to the other, quantified by an average angle $\bar{\varphi}$. It is considered that the director orientation at the LC-polymer interface varies over the illuminated area of the sample, implying the presence of defects in the LC layer that will not be explicitly addressed by our simplified analysis. The director field is parametrized as follows:

$$\vec{n}(z) = \cos\theta(z)\cos\phi(z)\hat{e}_x + \cos\theta(z)\sin\phi(z)\hat{e}_y + \sin\theta(z)\hat{e}_z, \tag{1}$$

where $\theta(z)$ and $\varphi(z)$ are functions to be determined from the minimization of the free energy per unit area of the nematic slab. This minimization leads to a set of coupled Euler-Lagrange equations [18] that after a first integration become

$$\begin{aligned}
&\left[g_1(\theta) - \frac{1}{4}\frac{g_2(\theta)^2}{g_3(\theta)}\right]\left(\frac{d\theta}{dz}\right)^2 + \frac{1}{4}\frac{D_z^2}{g_1(\theta)} + \frac{1}{4}\frac{c_1^2}{g_4(\theta)} = c_2,\\
&g_1 \equiv \frac{1}{2}[K_1\cos^2(\theta) + K_3\sin^2(\theta)],\quad g_2 \equiv \frac{e_1+e_3}{2}\sin(2\theta),\\
&g_3 \equiv -\frac{1}{2}[\Delta\varepsilon\sin^2(\theta) - \varepsilon_\perp],\\
&g_4 \equiv \cos^2(\theta)\frac{1}{2}[K_2\cos^2(\theta) + K_3\sin^2(\theta)],\\
&\frac{d\phi}{dz}\cos^2(\theta)[K_2\cos^2(\theta) + K_3\sin^2(\theta)] = c_1,\\
&\frac{e_1+e_3}{2}\sin(2\theta)\frac{d\theta}{dz} + [\Delta\varepsilon\sin^2\theta + \varepsilon_\perp]E_z = D_z,
\end{aligned} \tag{2}$$

where the K_i are the Frank elastic constants; $\Delta\varepsilon = \varepsilon_{||} - \varepsilon_\perp$ and $\varepsilon_{||}$, $\varepsilon_\perp$ are the principal values of the dielectric permittivity tensor of the nematic; e_1 and e_3 are the flexoelectric coefficients; c_1, c_2 are integration constants [18]; and D_Z is the electric displacement vector component. E_Z is the electric field. In obtaining (2) it was considered that the electric potential in the nematic slab only depends on z; the electric field is then directed along z and it is related to the z component of the electric displacement in the cell D_z that is then constant. It is then possible to solve the system of equations (2) along with the equation for the total voltage applied to the cell and determine numerically the electric displacement D_z, $\theta(z)$, and $\varphi(z)$ for each applied voltage V.

From the value of D_z for each applied voltage V we determine the sample capacitance that was also experimentally measured along with the light transmission coefficient,

$$C = \frac{D_z A}{V}, \tag{3}$$

where A is the active sample surface area. Both the sample capacitance and the light transmission coefficient as a function of the applied voltage were fitted to the experimental results.

We now address the light transmission calculation. From Kirchhoff's diffraction theory [14] the field at the detector $\vec{u}_d$ is

$$\vec{u}_d = -\frac{i}{\lambda}\int_S \vec{u}_S\frac{e^{ikr}}{r}\,dS, \tag{4}$$

where i is the imaginary unit, λ is the wavelength, S is the illuminated outer surface of the device facing the detector, $\vec{u}_S$ is the field at S, k is the light wave vector in free space, and r is the distance from the surface element dS to the detector. The light intensity at the detector is proportional to the modulus square of $\vec{u}_d$; its spatial average over the sample surface equates to

$$I \propto \frac{1}{(\lambda l)^2}\int_S\int_{S'}\langle u_S u_{S'}^*\rangle\frac{e^{\frac{ik}{2l}(\rho^2-\rho'^2)}}{r}dSdS', \tag{5}$$

where l is the distance from the sample to the detector and ρ and ρ' are the radial distances in the sample surface from the origin at the sample surface center to the surface elements dS and dS'. The brackets indicate a surface average. In our experiment we have separated the field $\vec{u}_d$ in its components parallel and perpendicular to the incident linearly polarized

field in the sample using a polarizing beam splitter cube, giving rise to $I_{||} \propto u_{d||} u^*_{d||}$ and $I_{\perp} \propto u_{d\perp} u^*_{d\perp}$ with the latter showing always negligible values relative to the former. The light transmission coefficient measured in our experiment corresponds to the ratio $I_{||}/I_{||o}$ where $I_{||o}$ is the intensity reaching the detector in the absence of the scattering cell. Fresnel factors [16] at the four glass interfaces of the optical cell are later included in the calculation of the final value for $I_{||}$.

The field $\vec{u}_S$ is calculated using the Jones matrices formalism [19] since light is crossing the stratified device containing a birefringent nematic LC layer at normal incidence.

In the optical analysis with the Jones matrices formalism the LC layer is considered to be divided into sublayers within which the director is uniform. The evolution of the director in the nematic layer when going from one polymer surface to the other, corresponding to different anchoring easy directions that change over the polymer surfaces from point to point, may imply some degree of twist of the director field that will be quantified by an average rotation angle $\pm\bar{\varphi}$ and a variance $\delta\varphi^2$. For simplicity three layers were considered, giving rise to the following relation between the incident field $\vec{u}_i$ and the field $\vec{u}_S$:

$$\begin{bmatrix} u_{sx} \\ u_{sy} \end{bmatrix} = \begin{bmatrix} e^{i\delta_p/2} & 0 \\ 0 & e^{i\delta_p/2} \end{bmatrix} R(\phi_3) \begin{bmatrix} e^{i\delta_{3\perp}} & 0 \\ 0 & e^{i\delta_{3||}} \end{bmatrix} R^{-1}(\phi_3) R(\phi_2) \begin{bmatrix} e^{i\delta_{2\perp}} & 0 \\ 0 & e^{i\delta_{2||}} \end{bmatrix} \times R^{-1}(\phi_2) R(\phi_1) \begin{bmatrix} e^{i\delta_{1\perp}} & 0 \\ 0 & e^{i\delta_{1||}} \end{bmatrix} R^{-1}(\phi_1) \begin{bmatrix} e^{i\delta_p/2} & 0 \\ 0 & e^{i\delta_p/2} \end{bmatrix} \begin{bmatrix} u_{ix} \\ u_{iy} \end{bmatrix}, \quad (6)$$

where R is a rotation matrix $R(\phi) = \left[\begin{smallmatrix} \cos(\phi) & \sin(\phi) \\ -\sin(\phi) & \cos(\phi) \end{smallmatrix}\right]$ and $\phi_2 = \phi_1 + \frac{\varphi}{2}$, $\phi_3 = \phi_1 + \varphi$.

The angle $\phi_1 = \pi/2 - \beta$, where β is the angle between the electric field of the incoming light wave and the projection of the nematic director on the sample surface, and consequently ϕ_2 and ϕ_3, are considered to vary randomly over the cell's surface with a characteristic correlation length l_ϕ. $\delta_{i\perp}$ and $\delta_{i||}$ are the phase shifts experienced by the light waves with the electric field respectively orthogonal to and in the plane of the nematic director in the sublayer i and also vary randomly over the sample surface due to the random nature of the polymer-LC interfaces. δ_p is the phase shift in the polymer layers. This random nature of $\delta_{i\perp}$, $\delta_{i||}$, and δ_p is quantified considering that the LC layer thickness has an average value $\bar{z}_{LC}$ and fluctuates over the sample surface with a correlation length l_Z and a variance $(\Delta z_{LC})^2$. $\Delta z_{LC} \equiv \sqrt{\langle (z_{LC} - \bar{z}_{LC})^2 \rangle}$ is the root mean square roughness amplitude of the LC-polymer interface. Due to the presence of random variations of z_{LC}, ϕ_1, and φ over the sample surface with correlation lengths l_Z, l_ϕ, and l_φ, the light intensity at the detector includes an averaging over the distribution of these variables indicated by the brackets in Eq. (5); the details are given in the Appendix.

Figures 2 and 3 present the light transmission and capacitance applied field dependences for one of the cells studied along with fits from the model, respectively.

We used known and fitting parameters in the model. The known parameters include the LC refraction indices $n_{||} = 1.736$, $n_\perp = 1.511$ [20] and dielectric constants $\varepsilon_{||} = 19\varepsilon_0$, $\varepsilon_\perp = 5.2\varepsilon_0$ [21]; the wavelength of the visible light used $\lambda = 632.8$ nm; the distance from the sample to the detector $l = 0.2$ m; the glass index of refraction $n_{glass} = 1.51$; the LC and polymer layer thicknesses $l_{LC} = 10\ \mu$m, $l_p = 2\ \mu$m; the device active area $S = 5.64$ cm^2; and the LC Frank elastic constants $K_{11} = 11.1$ pN, $K_{22} = 6.0$ pN, $K_{33} = 17.1$ pN [21]. The sum of the flexoelectric coefficients $e_1 + e_3$ (not known for E7 which is a mixture of three cyanobiphenyl LCs) was approximated by the value reported for 5CB, $e_1 + e_3 = -8.4$ pC/m [22]. The fitting parameters include the root mean square roughness amplitude, $\sqrt{\langle \Delta z^2_{LC} \rangle} = 1.95\ \mu$m; the polymer layer index of refraction $n_p = 1.49$ and dielectric constant $\varepsilon_p = 2.32\varepsilon_0$; the average director twist angle $\bar{\varphi} = \pm 0.6$ rad and its distribution width $\Delta\varphi = 2.93$ rad; the correlation lengths $l_Z = 1\ \mu$m, $l_\phi = 1\ \mu$m, and $l_\varphi = 0.9\ \mu$m; and the director pretilt at

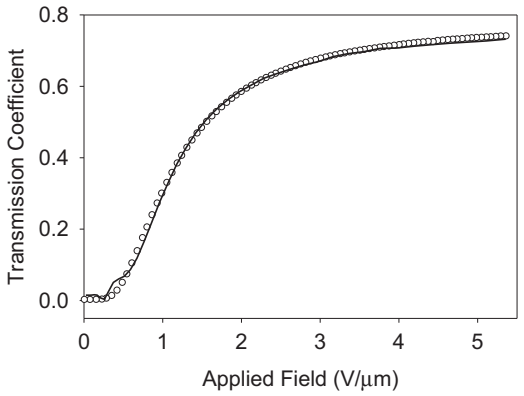

FIG. 2. Applied field dependence of the transmission coefficient. (Circles) CA data; (continuous line) model fit.

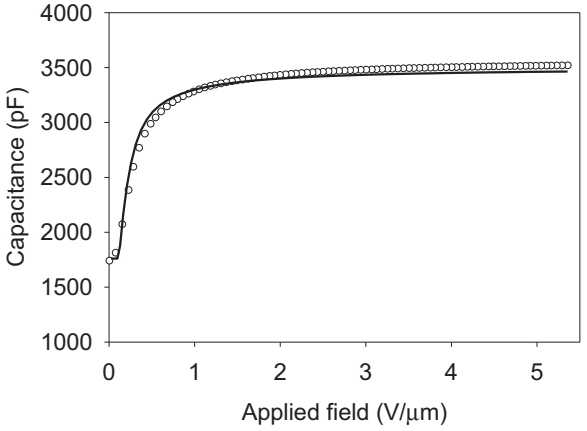

FIG. 3. Applied field dependence of the sample capacitance. (Circles) CA data; (continuous line) model fit.

the LC-polymer layer interfaces $\theta_1 = 0.0$ rad. Regarding the fittings shown in Figs. 2 and 3 we see that in general they reproduce well the experimental results but a small irregularity on the theoretical light transmission curve can be observed for low voltages. This irregularity is reminiscent of the strong interference modulations that appear in the light transmission as a function of applied voltage when the director experiences no twist on going from one face to the other of the optical cell [23]. They arise from the constructive interference between the ordinary and extraordinary rays traveling through the LC medium; these interference maxima are strongly attenuated by the twisting of the director within the LC material. The roughness of the polymer-LC interfaces inducing random local LC director variations (not included in the simulation) is also a strong contributor to the suppression of the interference modulations referred to above.

III. CONCLUSIONS

The overall good quality of the fits indicates that the model captures the main aspects of the device's behavior, with the roughness of the LC polymer interfaces playing a central role in defining the optical characteristics of the device, in particular, the scattering in the OFF state. The simultaneous fitting of both the light transmission coefficient and the cells' capacitance imposes strong constraints on the model, contributing significantly to a precise definition of the director response to the applied voltage and its role in the optical response of the device. This work shows that the composite devices using nematic liquid crystals and cellulose based polymeric micro- and nanofibers obtained by electrospinning constitute efficient electrically switchable light-scattering shutters capable of achieving high contrast and high transmissions in the ON state suitable for low loss optical valves.

ACKNOWLEDGMENTS

We acknowledge support from the Portuguese Science and Technology Foundation (FCT/MCT) through Projects No. PTDC/CTM-POL/1484/2012, No. PTDC/FIS/110132/2009, and No. PEst-C/CTM/LA0025/2011 (Strategic Project No. LA 25-2011-2012).

APPENDIX

Determination of the average $\langle u_S u^*_{S'}\rangle$: The field vector u_S at S can be written in accord with the result of Eq. (6) as

$$u_S[\phi_1(\vec{r}),\varphi(\vec{r}),z_{\rm LC}(\vec{r})] = \sum_{j=1}^{2^{(2n-1)}} f_j[\phi_1(\vec{r}),\varphi(\vec{r}),z_{\rm LC}(\vec{r})] = \sum_{j=1}^{2^{(2n-1)}} f_{aj}(\phi_1,\varphi) f_{bj}(z_{\rm LC}), \quad \text{(A1)}$$

where the quantities $\phi_1(\vec{r}),\varphi(\vec{r}),z_{\rm LC}(\vec{r})$ in Eq. (A1) are random variables on the sample surface position indicated by $\vec{r}$. $n = 3$ is the number of layers considered in our case. The average $\langle u_S u^*_{S'}\rangle$ is then given by

$$\langle u_S(\phi,\varphi,z_{\rm LC}) u^*_{S'}(\phi',\varphi',z'_{\rm LC})\rangle = \left\langle \sum_{j=1}^{2^{(2n-1)}} f_{aj}(\phi_1,\varphi) f_{bj}(z_{\rm LC}) \sum_{m=1}^{2^{(2n-1)}} f^*_{am}(\phi'_1,\varphi') f^*_{bm}(z'_{\rm LC}) \right\rangle. \quad \text{(A2)}$$

Considering now the random variables ϕ_1, φ, z_{LC} to be independent we obtain

$$\langle u_S(\phi,\varphi,z_{cl}) u^*_{S'}(\phi',\varphi',z'_{\rm LC})\rangle = \sum_{j=1}^{2^{(2n-1)}} \sum_{m=1}^{2^{(2n-1)}} \langle f_{aj}(\phi_1,\varphi) f^*_{am}(\phi'_1,\varphi')\rangle \langle f_{bj}(z_{\rm LC}) f^*_{bm}(z'_{\rm LC})\rangle. \quad \text{(A3)}$$

The second average in Eq. (A3) is calculated as follows:

$$\langle f_{bj}(z_{\rm LC}) f^*_{bm}(z'_{\rm LC})\rangle = \langle f_{bj}(z_{\rm LC})\rangle\langle f^*_{bm}(z'_{\rm LC})\rangle + \langle\!\langle [f_{bj}(z_{\rm LC}) - \langle f_{bj}(z_{\rm LC})\rangle][f^*_{bm}(z'_{\rm LC}) - \langle f^*_{bm}(z'_{\rm LC})\rangle]\rangle\!\rangle, \quad \text{(A4)}$$

where it is considered that the correlation indicated by the second term decays exponentially in the sample plane with the distance between the points characterized, respectively, by the variables with and without prime and located at $\vec{r}$ and $\vec{r}'$. The average becomes

$$\langle f_{bj}(z_{\rm LC}) f^*_{bm}(z'_{\rm LC})\rangle = \langle f_{bj}(z_{\rm LC})\rangle\langle f^*_{bm}(z_{\rm LC})\rangle + [\langle f_{bj}(z_{\rm LC}) f^*_{bm}(z_{\rm LC})\rangle - \langle f_{bj}(z_{\rm LC})\rangle\langle f^*_{bm}(z_{\rm LC})\rangle] e^{-\frac{|\vec{r}-\vec{r}'|}{l_{z_{\rm LC}}}}. \quad \text{(A5)}$$

The average $\langle f_{bj}(z_{\rm LC})\rangle$ is in accord with the result of Eq. (6) given by

$$\langle f_{bj}(z_{\rm LC})\rangle = \langle e^{i\{\delta_{1j}(z_{\rm LC})+\delta_{2j}(z_{\rm LC})+\delta_{3j}(z_{\rm LC})+\delta_p(z_{\rm LC})\}}\rangle,$$

and defining

$$X_j \equiv \{\delta_{1j}(z_{\rm LC}) + \delta_{2j}(z_{\rm LC}) + \delta_{3j}(z_{\rm LC}) + \delta_p(z_{\rm LC})\},$$

which is considered also to be a Gaussian random variable over the sample surface due to the roughness of the polymer-LC interfaces. The average $\langle f_{bj}(z_{\rm LC})\rangle$ is evaluated as

$$\langle f_{bj}(z_{\rm LC})\rangle = \langle e^{iX_j}\rangle = e^{i\langle X_j\rangle} e^{-\frac{1}{2}\langle (X_j-\langle X_j\rangle)^2\rangle}. \quad \text{(A6)}$$

The phase shifts $\delta_{mj}(z_{\rm LC})$ included in X_j can assume one of two values, $\delta_{mj}(z_{\rm LC}) = \{\frac{k_o \bar{n}_{em} z_{{\rm LC}m}}{k_o n_o z_{{\rm LC}m}}\}$, depending upon the value of the index j; k_o is the light wave vector in free space, n_o is the LC ordinary refraction index, $\bar{z}_{{\rm LC}m}$ is the average thickness of the LC m sublayer, and $\bar{n}_{em}$ is the average LC effective extraordinary refraction index in the sublayer m given by $\bar{n}_{em} = \frac{1}{\bar{z}_{{\rm LC}m}} \int_{\bar{z}_{{\rm LC}m}} \frac{n_e n_o}{\sqrt{n_e^2 \sin^2(\theta) + n_o^2 \cos^2(\theta)}}\, dz$. The average

$\langle X_j \rangle$ becomes

$$\langle X_j \rangle = k_o \left\{ \bar{z}_{\mathrm{LC1}} \begin{Bmatrix} \bar{n}_{e1} \\ n_o \end{Bmatrix}_j + \bar{z}_{\mathrm{LC2}} \begin{Bmatrix} \bar{n}_{e2} \\ n_o \end{Bmatrix}_j + \bar{z}_{\mathrm{LC3}} \begin{Bmatrix} \bar{n}_{e3} \\ n_o \end{Bmatrix}_j + \bar{z}_p n_p \right\}$$

where $\bar{z}_{\mathrm{LC3}} = \bar{z}_{\mathrm{LC1}}$, $\bar{z}_p$ is the polymer layers' total average thickness, and $\bar{z}_{\mathrm{LC1}}$ is determined by minimizing the average square difference between $\phi(z)$ determined from Eq. (2) and $\phi(z)$ considered in the LC layered structure yielding the equation $\phi(\bar{z}_{\mathrm{LC1}}) = \frac{\bar{\varphi}}{4}$. The average $\langle\langle (X_j - \langle X_j \rangle)^2 \rangle\rangle$ is given by

$$\langle\langle (X_j - \langle X_j \rangle)^2 \rangle\rangle = k_o \left\langle \left\{ \Delta z_{\mathrm{LC1}} \begin{Bmatrix} \bar{n}_{e1} \\ n_o \end{Bmatrix}_j + \Delta z_{\mathrm{LC2}} \begin{Bmatrix} \bar{n}_{e2} \\ n_o \end{Bmatrix}_j + \Delta z_{\mathrm{LC3}} \begin{Bmatrix} \bar{n}_{e3} \\ n_o \end{Bmatrix}_j + \Delta z_p n_p \right\}^2 \right\rangle,$$

where $\Delta z_{\mathrm{LC}i} \equiv (z_{\mathrm{LC}i} - \bar{z}_{\mathrm{LC}i})$.

Considering now that $\Delta z_p = -\Delta z_{\mathrm{LC}}$ and the approximation $\Delta z_{\mathrm{LC}i} = \Delta z_{\mathrm{LC}} \frac{\bar{z}_{\mathrm{LC}i}}{\bar{z}_{\mathrm{LC1}} + \bar{z}_{\mathrm{LC2}} + \bar{z}_{\mathrm{LC3}}} = \Delta z_{\mathrm{LC}} \frac{\bar{z}_{\mathrm{LC}i}}{\bar{z}_{\mathrm{LC}}}$ we obtain

$$\langle\langle (X_j - \langle X_j \rangle)^2 \rangle\rangle = k_o \left\{ \frac{\bar{z}_{\mathrm{LC1}}}{\bar{z}_{\mathrm{LC}}} \begin{Bmatrix} \bar{n}_{e1} \\ n_o \end{Bmatrix}_j + \frac{\bar{z}_{\mathrm{LC2}}}{\bar{z}_{\mathrm{LC}}} \begin{Bmatrix} \bar{n}_{e2} \\ n_o \end{Bmatrix}_j + \frac{\bar{z}_{\mathrm{LC3}}}{\bar{z}_{\mathrm{LC}}} \begin{Bmatrix} \bar{n}_{e3} \\ n_o \end{Bmatrix}_j - n_p \right\}^2 \langle (\Delta z_{\mathrm{LC}})^2 \rangle.$$

The averages,

$$\langle f_{bj}(z_{\mathrm{LC}}) f^*_{bm}(z_{\mathrm{LC}}) \rangle = \langle e^{i\{\delta_{1j}(z_{\mathrm{LC}}) + \delta_{2j}(z_{\mathrm{LC}}) + \delta_{3j}(z_{\mathrm{LC}}) - \delta_{1m}(z_{\mathrm{LC}}) - \delta_{2m}(z_{\mathrm{LC}}) - \delta_{3m}(z_{\mathrm{LC}})\}} \rangle,$$

are calculated in a similar way.

The first average in Eq. (A3) involving the random variables ϕ_1 and φ was approximated as follows:

$$\langle f_{aj}(\phi_1,\varphi) f^*_{am}(\phi'_1,\varphi') \rangle = \int\int\int\int f_{aj}(\phi_1,\varphi) f^*_{am}(\phi'_1,\varphi') P_\varphi(\varphi,\varphi') P_\phi(\phi_1,\phi'_1) d\varphi d\varphi' d\phi_1 d\phi'_1,$$

with $P_\phi(\phi_1,\phi'_1) = P_{\phi I}(\phi'_1) P_{\phi II}(\phi_1|\phi'_1) = \frac{1}{2\pi} P_{\phi II}(\phi_1|\phi'_1)$ and $P_\varphi(\varphi,\varphi') = P_{\varphi I}(\varphi') P_{\varphi II}(\varphi|\varphi')$ with $P_{\varphi I}(\varphi')$ given by the sum of two Gaussian functions centered at the angles $\bar{\varphi}$ and $-\bar{\varphi}$ with standard deviations $\Delta\varphi$ $P_{\varphi I}(\varphi') = C[e^{-(\varphi'-\bar{\varphi}')^2/[2(\Delta\varphi')^2]} + e^{-(\varphi'+\bar{\varphi}')^2/[2(\Delta\varphi')^2]}]$, where C is a normalizing constant. The conditional probability density $P_{\phi II}(\phi_1|\phi_{1'})$ is approximated as the solution of a diffusion-type equation:

$$l_\phi \frac{\partial}{\partial r_d} P_{\phi II}(\phi_1|\phi'_1) = \frac{\partial^2}{\partial \phi_1^2} P_{\phi II}(\phi_1|\phi'_1),$$

with the boundary conditions $P_{\phi II}(\phi_1|\phi'_1)|_{r_d=0} = \delta(\phi_1 - \phi'_1)$ and $P_{\phi II}(\phi_1|\phi'_1)|_{r_d=\infty} = \frac{1}{2\pi}$ where $r_d \equiv |\vec{r} - \vec{r}'|$, leading to

$$P_\phi(\phi_1,\phi'_1) = P_{\phi I}(\phi'_1) P_{\phi II}(\phi_1|\phi'_1) = \frac{1}{2\pi} P_{\phi II}(\phi_1|\phi'_1) = \frac{1}{4\pi^2} \left\{ 1 + 2 \sum_{k>0} e^{-k^2 \frac{r_d}{l_\phi}} [\cos(k\phi_1)\cos(k\phi'_1) + \sin(k\phi_1)\sin(k\phi'_1)] \right\}.$$

Let us introduce now the partial averages,

$$F_{ajm}(\varphi,\varphi') \equiv \langle f_{aj}(\phi_1,\varphi) f^*_{am}(\phi_1,\varphi') \rangle_{\phi_1,\phi'_1} = \iint f_{aj}(\phi_1,\varphi) f^*_{am}(\phi'_1,\varphi') P_\phi(\phi_1,\phi'_1) d\phi_1 d\phi'_1,$$

to be used later. The conditional probability density $P_{\varphi II}(\varphi|\varphi')$ is a function of r_d and was approximated to a function that takes the limiting values $P_{\varphi II}(\varphi|\varphi') = \{ {}^{\delta(\varphi-\varphi')|_{r_d=0}}_{\frac{1}{2\pi}|_{r_d=\infty}} \}$ and for intermediate values of r_d gives rise to the final result for the first averages in Eq. (A3):

$$\langle f_{aj}(\phi_1,\varphi) f^*_{am}(\phi'_1,\varphi') \rangle = \iint F_{ajm}(\varphi,\varphi') P_\varphi(\varphi,\varphi') d\varphi d\varphi' = \left[\int F_{ajm}(\varphi,\varphi) P_{\varphi I}(\varphi) d\varphi - \frac{1}{2\pi} \iint F_{ajm}(\varphi,\varphi') P_{\varphi I}(\varphi) d\varphi d\varphi' \right] e^{-\frac{r_d}{l_\varphi}} + \frac{1}{2\pi} \iint F_{ajm}(\varphi,\varphi') P_{\varphi I}(\varphi) d\varphi d\varphi',$$

with the $F_{ajm}(\varphi,\varphi')$ introduced earlier. The explicit expressions for either the partial averages $F_{ajm}(\varphi,\varphi')$ or the first averages in Eq. (A3), $\langle f_{aj}(\phi_1,\varphi) f^*_{am}(\phi'_1,\varphi') \rangle$, are not presented due to their length.

[1] U. Bortolozzo, S. Residori, and J. P. Huignard, J. Phys. D: Appl. Phys. **41**, 224007 (2008).
[2] H. V. Craighead, J. Cheng, and S. Hackwood, Appl. Phys. Lett. **40**, 22 (1982).
[3] P. L. Almeida, M. H. Godinho, M. T. Cidade, and J. L. Figueirinhas, Mol. Cryst. Liq. Cryst. **368**, 121 (2001).
[4] P. L. Almeida, G. Lavareda,C. Nunes de Carvalho, A. Amaral, M. H. Godinho, M. T. Cidade, and J. L. Figueirinhas, Liq. Cryst. **29**, 475 (2002).
[5] P. L. Almeida, S. Kundu, J. P. Borges, M. H. Godinho, and J. L. Figueirinhas, Appl. Phys. Lett. **95**, 043501 (2009).
[6] P. S. Drzaic, J. Appl. Phys. **60**, 2142 (1986).
[7] H. S. Kitzerow, Liq. Cryst. **16**, 1 (1994).
[8] D. Coates, J. Mater. Chem. **5**, 2063 (1995).
[9] C. Chiccoli, P. Pasini, F. Sameria, and C. Zannoni, Phys. Lett. A **150**, 311 (1990).
[10] E. Berggren, C. Zannoni, C. Chiccoli, P. Pasini, and F. Semeria, Phys. Rev. E **49**, 614 (1994).
[11] E. Berggren, C. Zannoni, C. Chiccoli, P. Pasini, and F. Semeria, Phys. Rev. E **50**, 2929 (1994).
[12] M. Rotunno, M. Buscaglia, C. Chiccoli, F. Mantegazza, P. Pasini, T. Bellini, and C. Zannoni, Phys. Rev. Lett. **94**, 097802 (2005).
[13] T. Bellini, M. Buscaglia, C. Chiccoli, F. Mantegazza, P. Pasini, and C. Zannoni, Phys. Rev. Lett. **88**, 245506 (2002).
[14] T. Bellini, M. Buscaglia, C. Chiccoli, F. Mantegazza, P. Pasini, and C. Zannoni, Phys. Rev. Lett. **85**, 1008 (2000).
[15] H. C. Van de Hulst, *Light Scattering by Small Particles* (Dover Publications, Inc., New York, 1981).
[16] M. Born and E. Wolf, *Principles of Optics*, 3rd ed. (Pergamon Press, Oxford, 1965).
[17] P. G. de Gennes and J. Prost, *The Physics of Liquid Crystals*, 2nd ed. (Clarendon Press, Oxford, 1993).
[18] F. M. Leslie, Mol. Cryst. Liq. Cryst. **12**, 57 (1970).
[19] S. Chandrasekhar, *Liquid Crystals*, 2nd ed. (Cambridge University Press, Cambridge, 1992).
[20] A. Fuh and O. Caporalleti, J. Appl. Phys. **66**, 5278 (1989).
[21] P. S. Drzaic and A. Muller, Liq. Cryst. **5**, 1467 (1989).
[22] L. M. Blinov, M. I. Barnik, M. Ozaki, N. M. Shtykov, and K. Yoshino, Phys. Rev. E **62**, 8091 (2000).
[23] H. Gruler, T. Scheffer, and G. Meier, Z. Naturforsch. **27a**, 966 (1972).